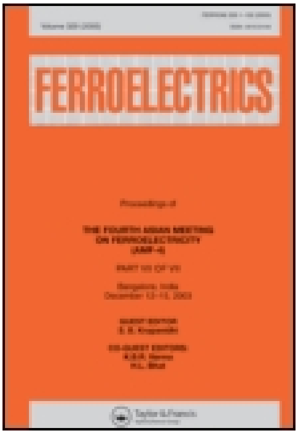

Ferroelectrics
Publication details, including instructions for authors and subscription information:
http://www.tandfonline.com/loi/gfer20

Internal stress and structural geometry calculations of a RAINBOW actuator

Wei Xiaoyong [a] , Li Guorong [a] & Chen Daren [a]
[a] Laboratory of Functional Inorganic Materials, Shanghai Institute of Ceramics, Shanghai, 200050, P.R., China
Published online: 09 Mar 2011.

Ferroelectrics, 1999, Vol. 234(1-4), pp. 235-250
Reprints available directly from the publisher
Photocopying permitted by license only

INTERNAL STRESS AND STRUCTURAL GEOMETRY CALCULATIONS OF A RAINBOW ACTUATOR

WEI XIAOYONG, LI GUORONG and CHEN DAREN*

(Laboratory of Functional Inorganic Materials, Shanghai Institute of Ceramics, Shanghai 200050, P.R.China)

(Received May 27, 1999)

The performance of the Reduced And INternally Biased Oxide Wafer (RAINBOW) actuator developed by Haertling, as explained by many authors, mainly owes to the special behaviors of domains under the high internal stress status. The finite element method (FEM) was the one used by Haertling's group to simulate the internal stress in RAINBOW and its dome shape of RAINBOW, and their FEM simulation results can explain some experimental results of RAINBOW actuator. In this paper, a simple model is presented to evaluate the internal stress and dome shape of RAINBOW actuator on the basis of the two step formation of RAINBOW structure. The internal radius stress and structural deformation of RAINBOW actuators with different geometrical dimensions were calculated by the present model. The results show good agreements with that of FEM simulation by Haertling and by us. Moreover, the optimal thickness ratio (the reduced layer/total) of the RAINBOW actuator, which represents the highest displacement induced by an electric field in its symmetric axial, can be directly determined from this model (the optimal thickness ratio is about 0.33, close to that calculated by FEM). This model has a clear physical meaning, explaining easily the non-uniform stress in the RAINBOW actuators from the physical point view, and is very useful for the RAINBOW actuator designs. These advantages are not so easily obtained by FEM. From the point of view of the presented model, the origin of the strain-amplifying mechanism of the RAINBOW was preliminarily considered to be due to the structural geometry of the unique dome shape.

Keywords: RAINBOW actuator; internal stress; FEM

1. INTRODUCTION

It was first reported in 1994 that the RAINBOW (Reduced And Internally Biased Oxide Wafer) actuator features ultrahigh displacement under an applied electric field and moderate load capacity[1]. As described there, this device was prepared by chemically single-side reducing one high lead-containing piezoelectric

* Correspondence Author.

ceramic wafer, therefore generating a bi-layer structure of reduced metallic cermet layer bonded with unreduced ceramics layer. After cooling down, an unique dome shape structure come into being due to thermal expansion mismatch between two layers.

The good performances of RAINBOW actuators had attracted researchers' interests and much work has been done to evaluate properties of this new type actuator. Haertling, Furman and Elissalde have learned about the chemical reduction behavior of the applied materials, and structural, compositional, electromechanical and resonant properties of this actuator[2–7]. Li has introduced special kinds of antiferroelectric RAINBOW actuators[8]. Dausch has investigated ferroelectric polarization fatigue and asymmetric 90° domain switching behavior of the RAINBOW actuator[9,10].

Although lots of papers related to RAINBOW have been published, few of them have touched on the internal stress distribution and electric field induced strain-amplifying mechanism[11]. In this paper, approximate analytic calculations and finite element analysis were employed to complete such objectives. Results of these two methods show good agreement.

2. APPROXIMATE ANALYTIC CALCULATION

The internal stress status in the RAINBOW actuator is difficult to accurately calculate due to its complex bi-layer dome shape and unknown material properties changing in the reduced layers. So, the most acceptable method is to get an approximate analytic result with some reasonable simplification.

First, although the RAINBOW actuator has some more sophisticated layer structures observed in its cross section, as reported by Ref. [5] and Ref. [12], we treat it as a bi-layer structure for convenience while introducing a minimum calculation error. Second, we assume the RAINBOW actuator as a slim bender along one diameter of itself instead of a dome shaped wafer. Such an assumption does not change the internal stress value along the radial direction, which is the stress component of most concern because the diameter of the wafer is much bigger than its thickness and the wafer is of axial symmetry in this situation. After these two simplifying steps, the structure of the RAINBOW actuator and its internal stress could be calculated by analytic deduction. The concept of internal stress or internal planar stress is referred to its radial stress component in this paper except for special cases.

Generally speaking, the internal stress of RAINBOW actuator is formed in two ways. One is the innerlayer normal stress induced by thermal expansion mismatch, and the other one is the bending stress produced by the thermal stress moment, which is related to the above innerlayer normal stresses. Approximate analytic calculation of internal stress could be done by adding these two parts together, and in this way the complexity of this problem is greatly decreased. It should also be pointed out that this kind of simplified calculation doesn't fit in with the situation of the two ends of the bender.

2.1 Normal stress induced by thermal expansion mismatch

Since there are different thermal expansion coefficients between the reduced and the unreduced layers, the inner-layer normal thermal stress was induced during the cooling process due to thermal expansion mismatch. That is, a tensile stress and a compressive stress exists in the reduced layer and the unreduced layer, respectively.

As shown in Fig. 1, L represents the length of the bender, R is the curvature radius, t_1, t_2 and t_0 are the thicknesses of reduced layer, unreduced layer and total bi-layer respectively(t_0=t_1+t_2).

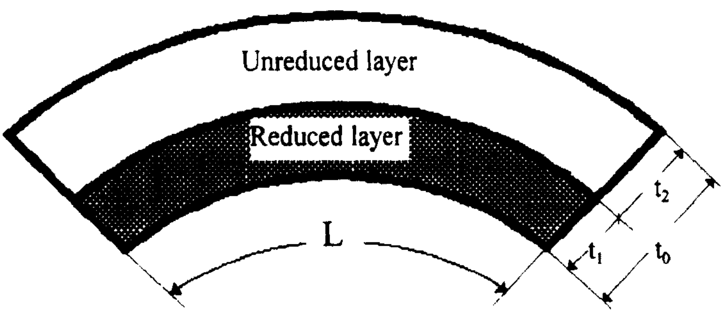

FIGURE 1 Structural schematic diagram of RAINBOW actuator

Before the bi-layer structure begins to bend after cool down (This means that even if there are stresses existing in the bender, we suppose it remains straight under a hypothetical situation), the inner-layer normal stresses should fit the following equation because the structure is free,

$$t_1 W\sigma_1 + t_2 W\sigma_2 = 0$$

where σ_1 and σ_2 represent the inner-layer stress of the reduced and unreduced layers respectively, W is the width of the slim bender. This equation can be simplified as

$$t_1\sigma_1 + t_2\sigma_2 = 0 \tag{1}$$

Based on Hucker's law, another equation can be derived from Fig. 2, (as shown in figure 2)

$$\sigma_1/\mathrm{Y} - \sigma_2/\mathrm{Y} = \Delta\mathrm{L}/\mathrm{L}$$

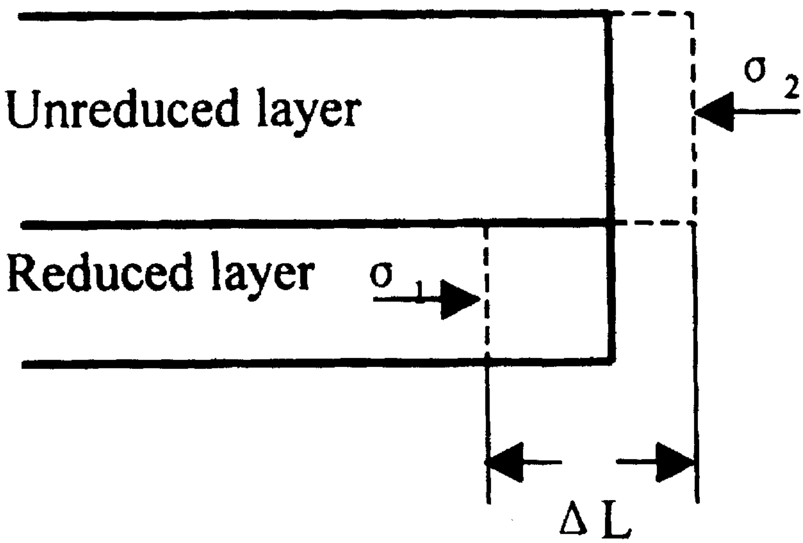

FIGURE 2 Thermal expansion mismatch normal stress and strain

From the definition of thermal expansion coefficient,

$$\Delta\mathrm{L}/\mathrm{L} = \Delta\mathrm{T}(a_1 - a_2) = \Delta\mathrm{T}\alpha_\mathrm{d}$$

where Y and α_1, α_2 are Young's modulus, thermal expansion coefficients of the reduced and unreduced layers respectively, and $\alpha_d = \alpha_1 - \alpha_2$. ΔT represents the difference between the temperature of reduction and R.T.. Here, we regard the piezoelectric ceramic as an isotropic material with the two layers having the same Young's modulus Y in order to simplify the resulting expression. Now we can obtain,

$$(\sigma_1 - \sigma_2)/\mathrm{Y} = \Delta\mathrm{T}a_\mathrm{d} \tag{2}$$

Solutions of Equ. 1 and Equ. 2 are

$$\sigma_1 = \mathrm{Y}\Delta\mathrm{T}a_\mathrm{d}\mathrm{t}_2/\mathrm{t}_0 \tag{3}$$

$$\sigma_2 = \mathrm{Y}\Delta\mathrm{T}a_\mathrm{d}\mathrm{t}_1/\mathrm{t}_0 \tag{4}$$

These equations show the relationships between the innerlayer normal stress and the parameters of the actuator and the material. As we can see, σ_1 is positive while σ_2 is negative, indicating that the tensile and compressive stresses exist in the reduced and the unreduced layers, respectively.

2.2 Bending stress induced by thermal stress moment

From Equ. 1, the absolute values of two the innerlayer normal thermal forces are equal. A pair of imagined external forces, which are equal to these two normal thermal forces respectively, must be applied on the ends of this bender to prevent the bi-layer structure from bending, this introduced as additional external forces. Because the bender is free, another pair of imagined reactive forces, which form a moment M, should also be accompanied with the former pair in order to actually simulate the practical situation. This moment M will cause the bender to be curved and introduce bending stresses into it. As shown in Fig. 3,

$$M = t_1 W \sigma_1 t_0/2 = t_2 W \sigma_2 t_0/2$$

with substitution of Equ. 3 or 4,

$$M = Y\Delta T a_d t_1 t_2 W/2 \tag{5}$$

FIGURE 3 Schematic diagram of imagined couple M and thermal bending stress σ_b

According to Navier's Law of pure bending cantilever[13], the bending stress of this bender is

$$\sigma_b = M(t_0/2 - t)/J$$

where t is a coordinate along the radius curvature, which starts at the unreduced layer surface. J is the bending stiffness of the cantilever ($J=Wt_0^3/12$). For simplification, we assume Young's moduli of the two layers are equal, that means, a neutral plane exists at the middle of the thickness. Then the expression of bending stress can be derived as below,

$$\begin{aligned}\sigma_b &= Y\Delta T\alpha_d t_1 t_2 W/2 \cdot (t_0/2 - t) \cdot 12/(W t_0^3) \\ &= 6Y\Delta T\alpha_d t_1 t_2 t_0^{-3}(t_0/2 - t) \qquad (6)\end{aligned}$$

It's clear that the bending stress σ_b decrease linearly from a positive value to a negative value along the axis of coordinate t.

2.3 Internal stress of the slim bender

With combination of the two parts of stresses above, the approximate value of internal stress can be expressed as

$$\sigma = \sigma_b + \sigma_t$$

σ_t means normal thermal stress. According to Equ. 3 and 4,

$$\sigma_t = \begin{cases} \sigma_1 = Y\Delta T\alpha_d t_2/t_0 & t_0 \geq t > t_2 \\ \sigma_2 = -Y\Delta T\alpha_d t_1/t_0 & t_2 > t \geq 0 \end{cases}$$

then the internal stress σ should be denoted as

$$\sigma = Y\Delta T\alpha_d[6t_1t_2t_0^{-3}(t_0/2 - t) + t_2t_0^{-1}] \quad t_0 \geq t > t_2$$

$$Y\Delta T\alpha_d[6t_1t_2t_0^{-3}(t_0/2 - t) - t_1t_0^{-1}] \quad t_2 > t \geq 0 \qquad (7)$$

Fig. 4 (a),(b),(c) show internal stress distributions under various thickness ratios (reduced layer thickness/total thickness) of 0.7, 0.5, 0.3 respectively, represent three kinds of typical situations, such as the thickness of reduced layer is bigger than, equal to or less than that of the unreduced layer. Whatever the thickness ratio is, the internal stress distribution curve is a two section line with continuous decrease along coordinate t and an abrupt jump at the interface between the two layers. For the discussed simplification reasons, this distributjon represents that of the centric internal planar stress of dome-shaped RAINBOW actuator.

What we are most concerned with is the internal stress of the unreduced layer, sinse piezoelectricity remains in this layer. In Fig. 4 (a) and (b), this stress is compressive; while in Fig. 4 (c), there is tensile stress in a region between the surface of the unreduced layer and a stress neutral plane, which exists in the unreduced layer. As we know, tensile stress along direction 1 is helpful to the extrinsic converse piezoelectric effect[11]. That means more lateral constrictive strain is engendered under a positive applied strong electric field. The effect of a compressive stress along direction 1 in a piezoelectric object is opposite, which

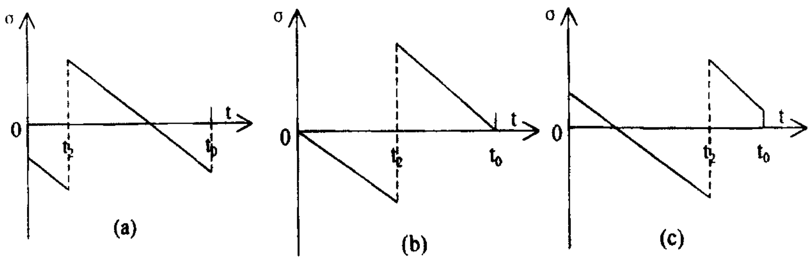

FIGURE 4 Approximate analytic results of distributions of internal stress

produces lateral strain loss. So when $t_1<t_2$, and because of the tensile stress, the unreduced layer being thicker than the reduced layer is preferable for a practical RAINBOW actuator with higher displacement properties.

2.4 Structural geometry deformation

As shown in Fig. 3, the vertical displacement x of the end of the bender is (based on mechanics of materials Equ. of a pure bending cantilever[13])

$$x = M/(2YJ) \cdot (L/2)^2$$

with substitution of Equ. 5

$$x = 3/4\Delta T\alpha_d L^2 t_0^{-3} t_1 t_2$$

The Dome height of a RAINBOW wafer equals that actuator's thickness plus the vertical displacement of the end of the wafer. In this approximate calculation, dome height h can be assumed as

$$h = t_0 + x$$

If $3/4L\ ^2 t_0^{-3} t_1 t_2$ is denoted as a proportional coefficient K, then the dome height should be

$$h = K\Delta T\alpha_d + t_0. \tag{8}$$

The curvature radius R is,

$$R = t_0^3/(6\Delta T\alpha_d t_1 t_2) \tag{9}$$

according to simple geometry relationships with x and L.

3. FEM SIMULATION OF INTERNAL STRESS AND STRUCTURAL DEFORMATION

FEM(Finite Element Method) analysis has become a powerful tool for engineering problems, especially for the stress and strain solution of complex structures, which are difficult to be solved by conventional analytic calculation.

A FEM software package of ALGOR (ver. 3.02) was employed to simulate the internal stress distribution and axial structural deformation of a RAINBOW actuator after cool down. A bi-layer-structured 3D wafer shaped FEM model of 380~456 units, which means 5~6 FEM layers with 76 units in each, were established as shown in Fig. 5. Figure 5 shows the dome-shaped-structure 3D model perspective of deformed RAINBOW. When the environment temperature decreases to R.T., the stresses appeared due to thermal expansion mismatch of the two layers. The upside and the downside FEM layers were the reduced and unreduced layers, respectively. The interface between them was located on one of the inner node planes according to the thickness ratio of the actuator. Units were of 6-node or 8-node types. After setting the appropriate material parameters, temperature was reduced from the stress free temperature (reducing temperature) to room temperature, during which a simulated stress appeared and the model began to dome just similar to the practical situation.

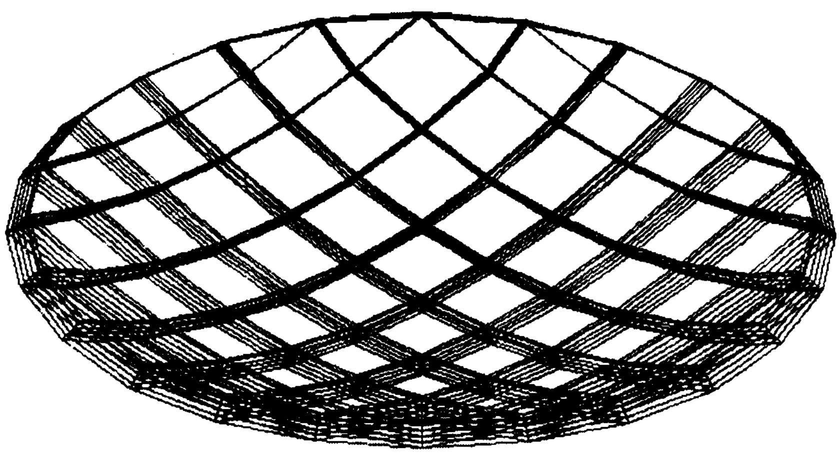

FIGURE 5 Perspective of deformed FEM 3D model

The Parameters of actuator and material used in this simulation are given in the following tables. The parameters of actuator are what we used in practice. The designated stress free temperature is 840°C.

TABLE I Parameters of RAINBOW actuator

No.	*Diameter (mm)*	*Thickness (mm)*	*Reduced layer thickness (mm)*	*Unreduced layer thickness (mm)*
1	26	1	0.05	0.95
2	26	1	0.1	0.9
3	26	1	0.15	0.85
4	26	1	0.2	0.8
5	26	1	0.25	0.75
6	26	1	0.3	0.7
7	26	1	0.4	0.6
8	26	1	0.5	0.5
9	26	1	0.6	0.4
10	26	1	0.7	0.3
11	26	1	0.8	0.2
12	26	1	0.9	0.1

TABLE II Parameters of applied material (The material parameters are cited from the appendix of Ref. [11])

Parameters	*Young's modulu ($\times 10^{10}Pa$)*	*Poisson's ratio*	*Effective thermal expansion coefficient*
Reduced layer	6.26	0.342	10×10^{-6}
Unreduced layer	7.42	0.374	5×10^{-6}

The most important stress component is the one along the radial direction in this situation because the diameter is much bigger than the thickness of the RAINBOW. As shown in Fig. 6, the distribution of internal planar stress along thickness of RAINBOW is very sophisticated. Figure 6 is a distribution diagram of centric planar stress along the thickness of an actuator with a thickness ratio of 0.3. It can be observed that the planar stresses oscillate between positive and negative values, i.e., tensile stress and compressive stress along the thickness direction. This oscillatory situation is similar to that of Fig. 4 (c). The FEM simulation and the analytic calculation basically agree with each other.

Fig. 7 shows the relationships between thickness ratio and the FEM calculated centric surface stresses of the upside surface (unreduced piezoelectric layer) and the downside layer (reduced layer). A conclusion from Fig. 7 is that the maxi-

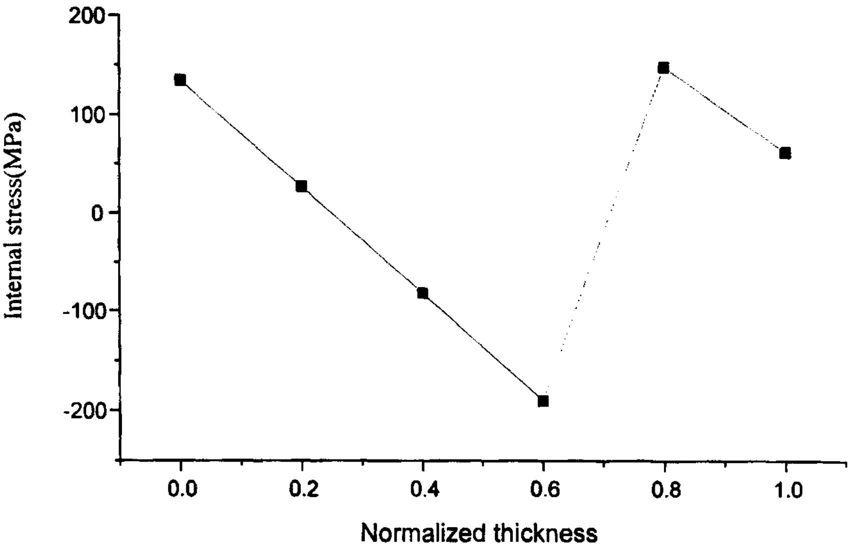

FIGURE 6 Internal planar stress distribution along thickness

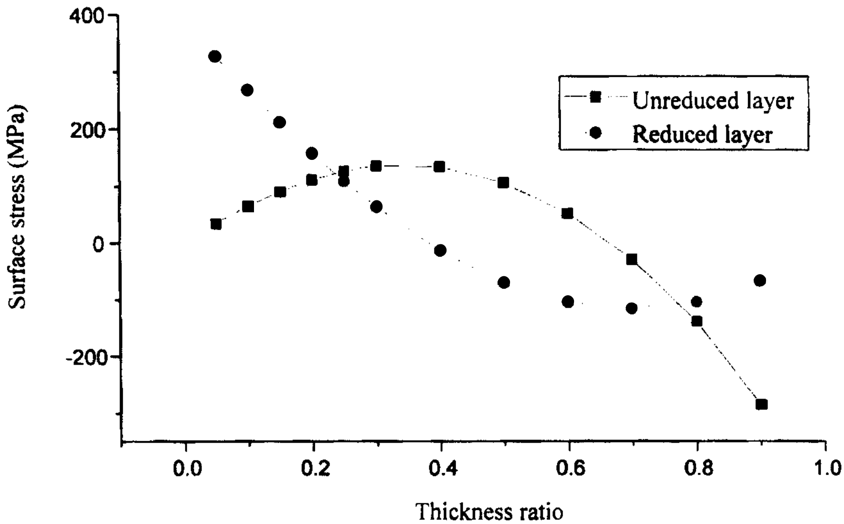

FIGURE 7 Surface planar stresses as a function of thickness ratio

mum tensile stress in the unreduced layer surface occurs at a thickness ratio of about 0.3. This enhances the extrinsic piezoelectric effect of piezoelectric ceramics under an applied strong electric field.

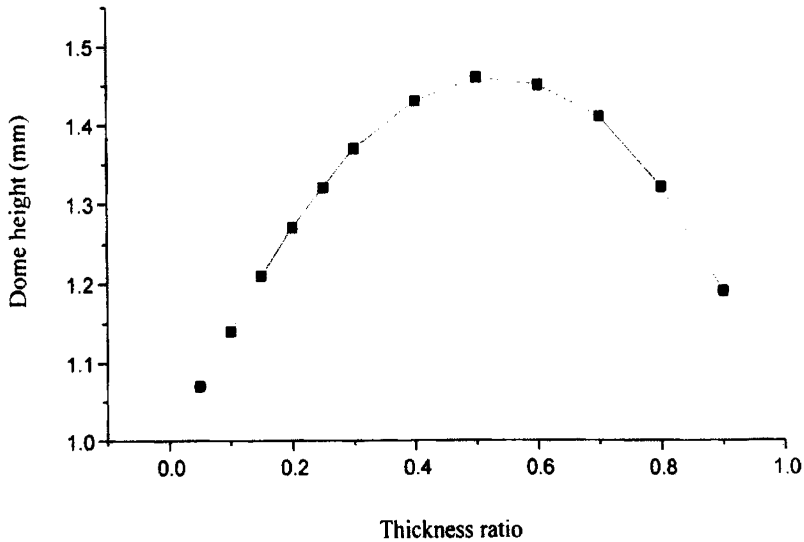

FIGURE 8 Dome height as a function of thickness ratio

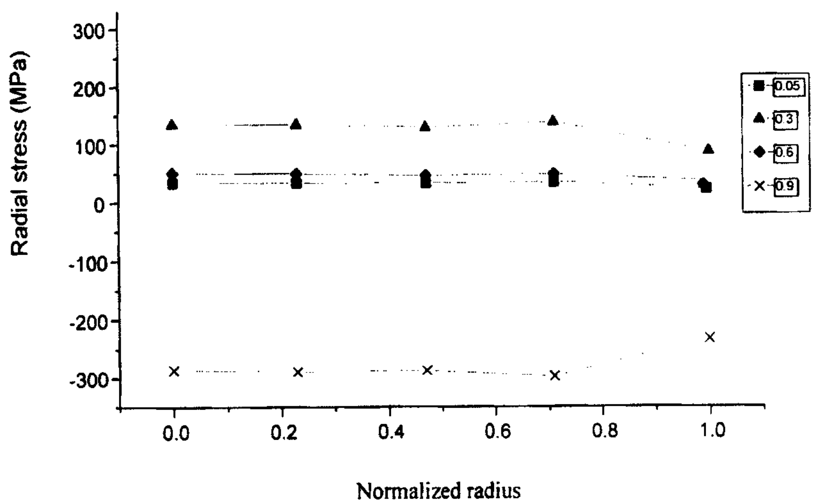

FIGURE 9 Planar stress distribution along unreduced layer with different thickness ratio

Fig. 8 shows the dome height of a RAINBOW when the thickness ratio increases, with the maximum value appearing at a thickness ratio of about 0.5. The curve is not completely symmetric because of the different Young's moduli used in the FEM model of the two layers.

Fig. 9 shows the distribution of planar stress on the unreduced layer surface, which is somewhat different with the FEM result of Li[11], who considered that the absolute stress values of the ends increased instead of going down to zero. Because the end of wafer is a free surface, this means the planar stress, which is vertical to the free surface, must be zero. The result in this paper seems to be more reasonable.

4. DISCUSSION

4.1 Internal planar stress agreement of analytic expression and FEM simulation

Equ. 7 is the analytic expression of internal planar stress, from which we can infer a variety of relationships.

For example, substitute t=0 into Equ. 7, we can get the expression of planar stress on the surface of the unreduced layer,

$$\begin{aligned}\sigma &= \mathrm{Y}\Delta\mathrm{T}\alpha_{\mathrm{d}}[6\mathrm{t}_1\mathrm{t}_2{\mathrm{t}_0}^{-3}(\mathrm{t}_0/2-0)-\mathrm{t}_1{\mathrm{t}_0}^{-1}] \\ &= \mathrm{Y}\Delta\mathrm{T}\alpha_{\mathrm{d}}(3\mathrm{t}_1\mathrm{t}_2{\mathrm{t}_0}^{-2}-{\mathrm{t}_0}^{-1}) \\ &= 3\mathrm{Y}\Delta\mathrm{T}\alpha_{\mathrm{d}}[1/9-(\mathrm{t}_1/\mathrm{t}_0-1/3)^2] \end{aligned} \tag{10}$$

This is a negative quadratic curve of variable $t_1/t_0$with the maximum value at $t_1/t_0=1/3$, i.e., when the thickness ratio is 0.33, the planar stress on the surface of the unreduced layer reaches a maximum. The optimal thickness ratio of the RAINBOW actuator is 0.33, where the unreduced layer has the maximum value of extrinsic lateral piezoelectric strain. This result is close to the FEM simulation, where the maximum appeared at the thickness ratio of 0.3.

If we substitute $t=t_1+t_2=t_0$ into Equ. 7, the expression of planar stress on the surface of the reduced layer could be deduced as,

$$\begin{aligned}\sigma &= \mathrm{Y}\Delta\mathrm{T}\alpha_{\mathrm{d}}[6\mathrm{t}_1\mathrm{t}_2{\mathrm{t}_0}^{-3}(\mathrm{t}_0/2-\mathrm{t}_0)+\mathrm{t}_2{\mathrm{t}_0}^{-1}] \\ &= \mathrm{Y}\Delta\mathrm{T}\alpha_{\mathrm{d}}(\mathrm{t}_2{\mathrm{t}_0}^{-1}-3\mathrm{t}_1\mathrm{t}_2{\mathrm{t}_0}^{-2}) \\ &= 3\mathrm{Y}\Delta\mathrm{T}\alpha_{\mathrm{d}}[(\mathrm{t}_1/\mathrm{t}_0-2/3)^2-1/3] \end{aligned} \tag{11}$$

Similar to the situation of t=0, a positive quadratic relationship indicates the variation of reduced layer surface planar stress under different thickness ratios. When t_1/t_0 equals 2/3, a minimum stress appears on the surface of the reduced layer.

To our surprise, these surface stresses are only related to three parameters, Y, ΔT α_d and the thickness ratio $t_1/t_0$and so do the internal layer planar stresses which are confirmed by detailed discussion of Equ. 7. It is difficult to understand that the other structure parameters such as diameter L and thickness t_0 have no effect on them. FEM simulation also proved this inference by changing such parameters of the model. The maximum tensile stress and minimum compressive stress of the actuator's two surfaces are constant under fixed Y, ΔT α_d and thickness ratio whatever L and t_0 are.

In the FEM simulation, the cited material parameters were used to calculate the stress distribution. If the same parameters are substituted into Equ. 10 and 11, figures 10 can be obtained.

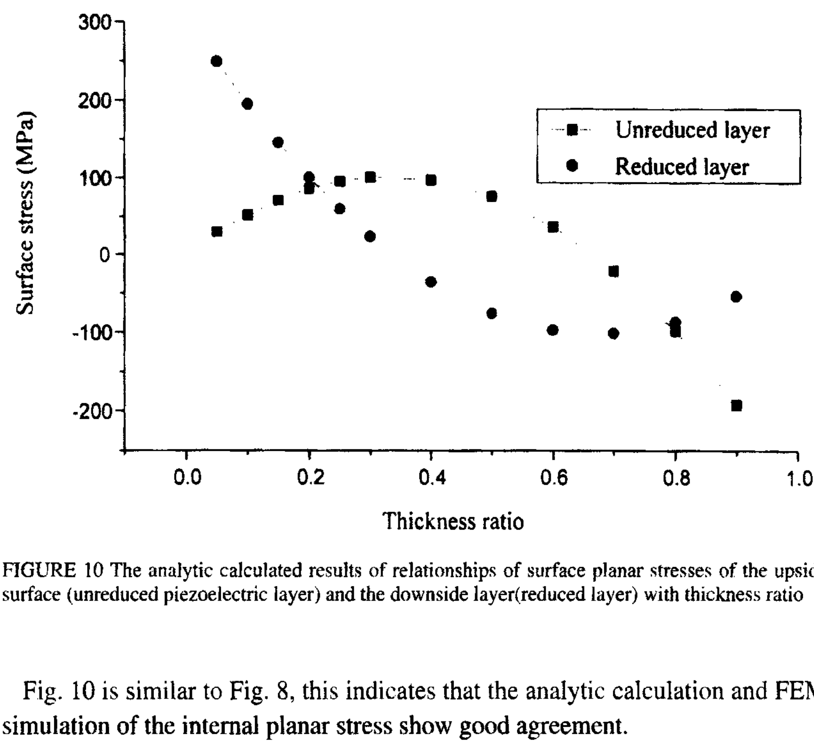

FIGURE 10 The analytic calculated results of relationships of surface planar stresses of the upside surface (unreduced piezoelectric layer) and the downside layer(reduced layer) with thickness ratio

Fig. 10 is similar to Fig. 8, this indicates that the analytic calculation and FEM simulation of the internal planar stress show good agreement.

4.2 RAINBOW dome height agreement of analytic expression and FEM simulation

Equ. 8 is the approximate analytic expression of RAINBOW dome height, where K is a function of t_1 and t_2 when the other parameters are constant. Figure 11 shows the relationship between dome height and thickness ratio with substitution of the same material parameters used in the FEM simulation. Maximum dome height appears at a thickness ratio of 0.5, which is about equal to that of FEM result. This curve is very close to that of Fig. 8, which shows the good agreement of structural deformation computation by two methods.

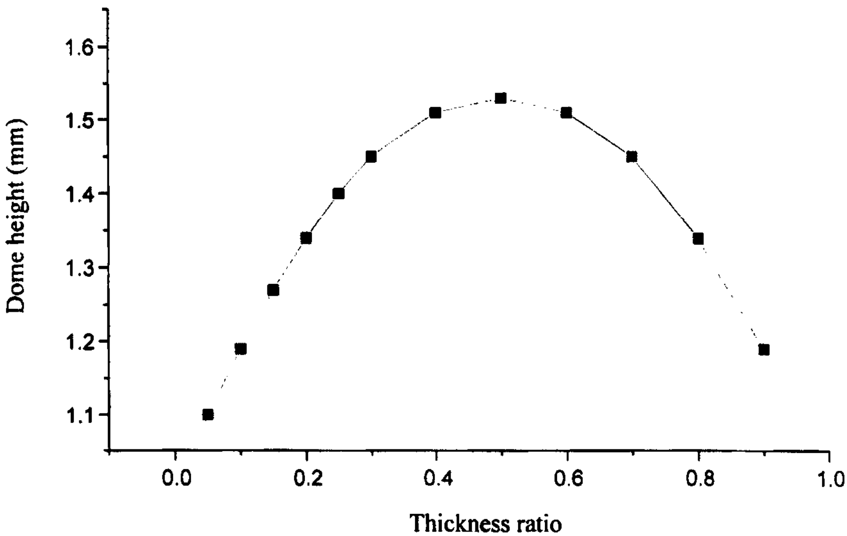

FIGURE 11 The analytic calculated results of dome height as a function of thickness ratio

4.3 Strain-amplifying mechanism

When considering the RAINBOW actuator, the most surprising thing is the ultra-high axial displacement. What is the origin, is it internal stress or dome shape? The strain-amplifying mechanisn will be preliminarily explained from the approximate analytic solution of the dome height.

Equ. 8 has shown out the relationship between dome height h and the other parameters. Among them, $\Delta T\ \alpha_d$ acts as a strain factor produced by the temperature change of the piezoelectric layer. So it's reasonable that the electrically induced strain is combined with this factor for calculating dome height change under applied electric field. Basically the equation of dome height change after applying the electric field can be expressed as

$$\Delta h = [K(\Delta T\alpha_d + s_1) + t_0] - [K\Delta T\alpha_d + t_0]$$
$$\Delta h = Ks_1 \qquad (12)$$

where $s_1 = s_i + bs_e$, represents the practical lateral strain of the unreduced layer, s_i and $s_e$are the intrinsic and extrinsic piezoelectric strains respectively, and b is an effective factor of interaction between non-uniform stress distribution and 90° ferroelectric domain rotation.

Here, s_i equals $d_{31}E_3$ (d_{31} is the intrinsic lateral piezoelectric constant, E_3 is the applied electric field along direction 3), and s_e, which relates to 90° domain rotation under strong electric field, could be measured by an experimental method under applied strong electric field. These two factors are now available while factor b is still difficult to decide yet. So it's impossible for us to write out the concrete relationships between s_l and material or structure parameters now. Maybe future work could decide it by experimental measurements.

Nevertheless, it is clearly shown in Equ. 12 how RAINBOW actuator can produce ultrahigh displacement. Acting as lateral strain factor, s_l has effects on symmetric axis displacement by multiplying with coefficient K. With typical parameters (L=26mm, t_0=0.3mm, t_1=0.1mm, t_2=0.2mm), K equals 376mm. Substitute it into Equ. 12, Δh can achieve an ultrahigh value for conventional piezoelectric actuator, 0.11 mm, if s_l equals 3×10^{-4}, which is a typical lateral strain data for piezoelectric ceramics under moderate applied electric field.

According to Equ. 12 and Equ. 8, symmetric axial strain s_h could be expressed as

$$s_h = \Delta h/h = s_l/(\Delta T a_d + t_0/K) \tag{13}$$

Typical values of the cited parameters above are, $\Delta T \alpha_d = 4.2 \times 10^{-3}$ and $t_0/K = 2.7 \times 10^{-3}$. s_h is much bigger than s_l. So a RAINBOW actuator can produce much higher strain along its axial direction than a normal piezoelectric actuator, because the denominator in Equ. 13, $\Delta T \alpha_d + t_0/K$ (6.9×10^{-3}), is much less than 1.

The ratios of s_h to s_l and s_l to s_i represent the contributions of structural geometry and internal stress distributions to the total strain-amplifying mechanism. It can be concluded that the former is much bigger than the latter. That means the structural geometry feature is the primary origin of the strain-amplifying mechanism of the RAINBOW actuator rather than internal stress distribution. The discussion above is only a preliminary explanation of the axial displacement and strain amplifying mechanism of RAINBOW actuator. It's the structural geometry instead of internal stress or its non uniform distribution that mainly brings out this feature.

5. CONCLUSION

The internal planar stress distribution and geometry deformation of RAINBOW actuator were calculated by means of approximate analytic calculation and FEM simulation. The maximum of tensile stress on the unreduced layer surface appeared at a thickness ratio of about 0.33, which benefited the extrinsic piezoelectric induced lateral strain of the unreduced layer. This thickness ratio was considered as the optimal structural parameter for ultrahigh displacement RAINBOW actuator. Analytic result shows that the maximum tensile stress and the minimum compressive stress have no relationship with the diameter and thickness of the actuator. The study of deformed dome height of a RAINBOW under applied electric field revealed that the origin of the strain-amplifying mechanism of a RAINBOW mainly arises from the structural geometry of its unique dome shape.

References

1. G. H. Haertling, Am. Ceram. Soc. Bull., **73** [1] (1994) pp. 93–96.
2. G. H. Haertling, Proc. 4thInt. SAMPE Elec. Conf., (1990) pp. 699–711.
3. G. H. Haertling, Ferroelectrics, **154** (1994) pp. 101–106.
4. G. Li. et. al., Ferroelectrics, **182** (1996) pp. 69–76.
5. C. Elissalde, et. al., J. Am. Ceram. Soc., **79** [8] (1996) pp. 2041–2048.
6. E. Furman, et. al., ISAF 94, (1994) pp. 146–149.
7. E. Furman, et. al., Ferroelectrics, **160** (1994) pp. 357–369.
8. G. Li, et. al., Ferroelectrics, **188** (1996) pp. 223–236.
9. D. E. Dausch, Ferroelectrics, **210** (1998) pp. 31–45.
10. D. E. Dausch, J. Am. Ceram. Soc., **80** [9] (1997) pp. 2355–2360.
11. G. Li, et. al., J. Am. Ceram. Soc., **80** [6] (1997) pp. 1382–1388.
12. X. Wei, et. al., J. Inorg. Mater. (Chinese), **14** [4] (1999) pp. 692-698.
13. S Timshinco, "Mechanics of Materials" (Chinese), (1964), Scientific Press, Beijing.